JOURNAL OF MATERIALS SCIENCE **39** (2004) 2547–2551

Characterization of a new relaxor perovskite of $Ba(Ni_{1/2}Mo_{1/2})O_3$

N. G. DURGE, M. S. NADKARNI
Physics Department, Patkar—Varde College, Goregaon, Mumbai 62, India

S. V. SALVI
Physics Department, Institute of Science, Madam Cama Road, Mumbai 32, India

A new perovskite $Ba(Ni_{1/2}\ Mo_{1/2})O_3$ with promising properties has been synthesized by the ceramic method. The XRD analysis indicates an ordered and hexagonal structure. The IR spectrum reveals the presence of Ni—O—Mo ordered bond. The room temperature relaxation spectra imply relaxor behavior of the ceramic. The "Debye term" corresponding to the space charge polarization exists at 8 KHz. The dielectric constant v/s temperature curve shows a diffuse phase transition at 950 K. The ceramic has a positive temperature coefficient of resistance near room temperature implying ferroelectric behavior.

A $(BB')\ O_3$ perovskites are known for relaxor behavior [1–3]. Perovskites in which the A-site is occupied by a rare earth/(Ba, Sr, or Ca) and the octahedral site is occupied by (Fe, Co, Ni etc.) are well investigated for their electrical and dielectric properties [4–6]. The synthesis of some molybdenum containing perovskites along with their structure (using X-ray diffractometry) have been reported [7]. However, no detailed investigation of other properties of these perovskites has been carried out. This has prompted us to synthesize $Ba(Ni_{1/2}\ Mo_{1/2})O_3$ (BNM) and investigate its structural and electrical properties.

Fine powders of AR grade $BaCO_3$, NiO (green) and MoO_3 were taken in 2:1:1 molecular weight proportion. The mixture was homogenized and presintered at temperatures below the melting point of MoO_3. Further, the heating was done progressively at 950, 1100 and 1200 °C for 24 h in each case. The structural information was obtained at all these temperatures by using the powder X-ray diffraction (XRD) technique on a Jeol-JDX-8030 diffractometer (Germany). The corresponding IR absorption spectra were recorded on a Perkin-Elmer1600 series FTIR spectrometer at room temperature from 400 to 1000 cm^{-1}.

The dielectric constants and loss of these samples were measured at 1 KHz by two-probe method using an LCR meter. The measurements were carried out from room temperature to 900 K. Also the relaxation spectra were recorded on 4284A precision LCR meter (Hewlett Packard) from 20 Hz to 1 MHz at room temperature. The DC resistivity was measured by the two-probe method from room temperature to 800 K. Finally, the I-V characteristic of the ceramic is measured at room temperature.

All XRD patterns were indexed according to hexagonal phase symmetry. Therefore, the XRD pattern and data of only sample, annealed at 1200 °C, are shown in Fig. 1 and Table I as a typical case. However, the lattice parameters of all three samples are compared in Table II.

It is interesting to note that lattice parameters are maximum at an annealing temperature of 1100 °C (Table II). However the particle size increases with annealing temperature. The slope of $\beta \cos\theta$ versus $\sin\theta$ indicates inhomogeneous (strained) growth of the unit cell, where β is the full width of the half maximum of the reflection [8]. Therefore, the magnitude of the slope is taken as a measure of inhomogeneity. The corresponding plot of material annealed at 1200 °C is shown in Fig. 2 as a typical case.

The IR absorption spectra of sample annealed at 1200 °C are depicted in Fig. 3. The corresponding band frequencies are tabulated in Table III. It is interesting to note that band frequencies shift to higher energy side by about 2.5% when annealing temperature increases (e.g., 790 cm^{-1} (at 1100 °C) to 819 cm^{-1} (at 1200 °C) and 545 cm^{-1} (at 1100 °C) to 570 cm^{-1} (at 1200 °C)). The higher frequency implies the larger effective charge on the cations, the smaller bond length or smaller mass of cation. The sample annealed at 1200 °C

TABLE I Comparison of observed and calculated d values of reflections of BNM at room temperature

d_{obs} (Å)	d_{cal} (Å)	I/I_o	hkl
3.351	3.349	100	212
3.200	3.205	33	301
2.841	2.838	83	220
2.781	2.790	21	221
2.409	2.410	18	313
2.320	2.342	39	116
2.089	2.090	36	225
2.009	2.010	31	207
1.876	1.876	21	414
1.698	1.700	26	334
1.642	1.643	27	407

TABLE II Structural properties of BNM at different annealing temperatures

Annealing temperature (°C)	Lattice constant		Particle size (Å)	Inhomogeneity (radians)	Percentage porosity
	a (Å)	c (Å)			
950	11.36	15.43	268	−0.61	–
1100	11.38	15.49	357	+0.081	13.2%
1200	11.35	15.46	462	+0.307	17.9%

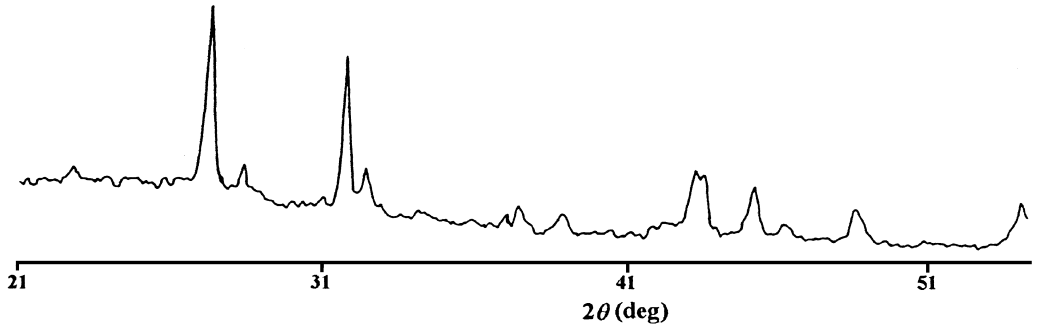

Figure 1 The XRD pattern of BNM measured at room temperature.

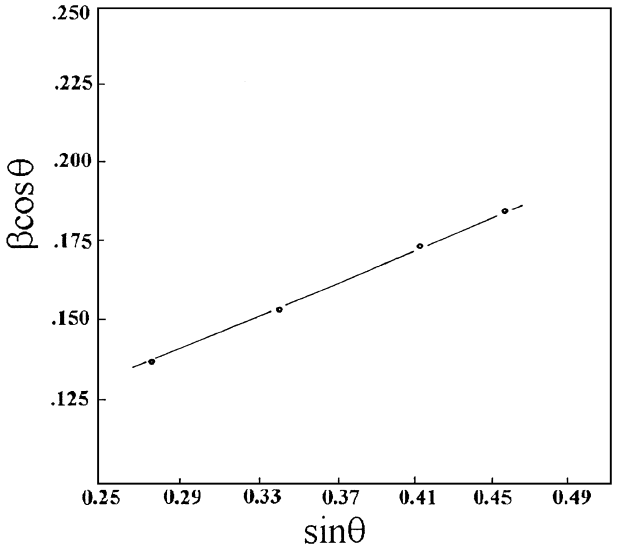

Figure 2 $\beta \cos\theta$ versus $\sin\theta$ for BNM.

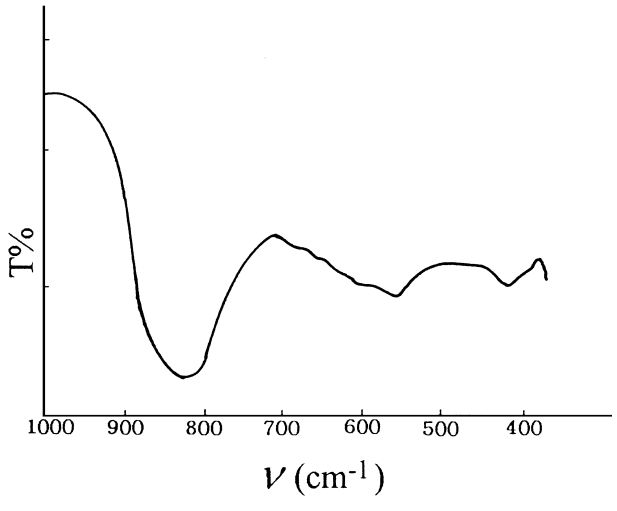

Figure 3 IR spectrum of BNM measured at room temperature.

has a lattice parameter smaller by about 0.3% than those of the sample annealed at 1100 °C. This means the corresponding bond length is smaller. Also, the sample at 1200 °C has strained growth. Hence it is concluded that the frequency shift is partly due to the strained bonds and partly due to the change in bond length.

Another interesting feature of the spectra is that the bands corresponding to the sample annealed at 1200 °C are broader. This implies increased disorder or inhomogeneity at 1200 °C as indicated earlier. The assignment of modes to different band frequencies [9, 10] is shown in Table III. The very intense band showing the presence of Ni—O—Mo bond implies an ordered unit cell. This explains the larger lattice parameters.

Fig. 4 shows the frequency dependence of the dielectric constant (k') and loss (k'') from 20 Hz to 1 MHz at room temperature. It is divided into three parts: (i) the low frequency region shows broad maximum, (ii) the mid frequency region shows a rapid fall with frequency, (iii) the high frequency region has a long tail. These features are comparable with curve obtained for model for different dielectric media designed for interfacial polarization [11–13]. However the broad low frequency maximum is indicative of a transition near room temperature.

The dielectric constants of samples annealed at 1100 and 1200 °C are compared at room temperature for two different frequencies in Table IV. The dielectric constant is observed to increase when annealing temperature increases. These trends are typical of a relaxor [1, 6].

The dielectric constant and loss of the ceramic annealed at 1200 °C are measured at 1 KHz from room temperature up to 1050 K. The curves are depicted in Fig. 5. They indicate that a transition below room temperature may exist [14]. Also, there is a broad diffused phase transition (DPT) around 950 K. The loss factor

TABLE III IR absorption frequencies and mode of assignment of bonds in BNM

Annealing temperature (°C)	Infrared frequencies (cm^{-1})	Mode of assignment
1100	790 (s) ν_1	Ni—O—Mo (str)
	545 (s, br) ν_2	Mo—O—Mo (str)
1200	819 (s) ν_1	Ni—O—Mo (str)
	570 (M, br) ν_2	Mo—O—Mo (str)
	427 (W) ν_3	Ni—O—Ni (ben)

s: strong; br: broad; M: medium, W: weak, str: stretching mode, ben: bending mode.

TABLE IV Room temperature dielectric constant

Annealing temperature (°C)	Dielectric constant k'	
	At 400 Hz	At 1 KHz
1100	148	100
1200	245	181

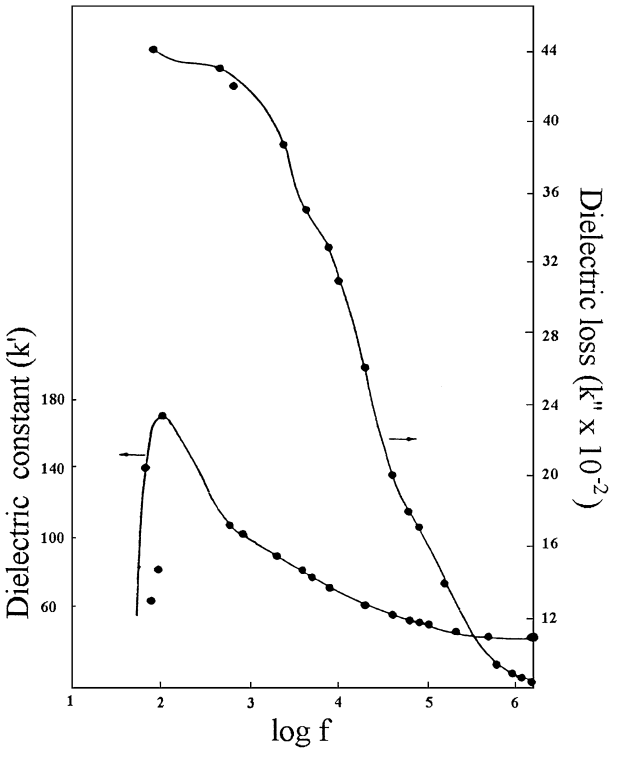

Figure 4 Dielectric constant k' and k'' versus logarithm of frequency for BNM.

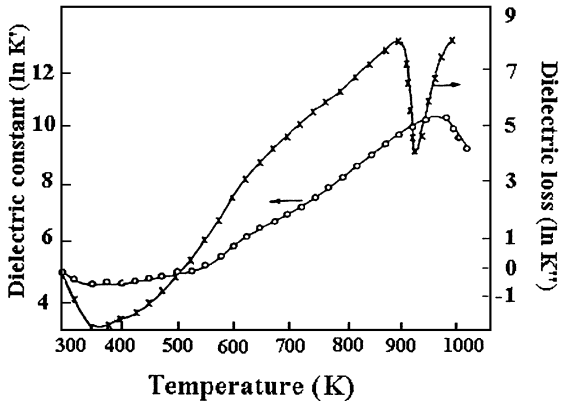

Figure 5 Dielectric constant k' and loss k'' at 1 KHz versus temperature for BNM.

behaves the same way as the dielectric constant with respect to temperature. However, discontinuities are more prominent.

A DPT has been explained on the basis of several factors [15–21]. However in the present case the DPT may be explained in the following manner. The smaller ionic radius of the Mo^{6+} ion is suitable for lowering the symmetry. Indeed, it causes the hexagonal ordering in this perovskite. However, the lower symmetry weakens interactions among the octahedra of different cations. This is evident from the small overall values of dielectric constant of this perovskite. Therefore, the ferroelectric domains caused by the ordering may be very very small in size and inhomogenously distributed in the material. This is responsible for the DPT in this perovskite.

Fig. 6 shows the plot for the sample annealed at 1200 °C of $\ln(1/k - 1/k'_{\max})$ versus $\ln(T - T_{\max})$. The slope of the plot indicates the diffuseness i.e., diffusivity (γ) of the phase transition [15]. The diffusivity is equal to 1 near room temperature and is equal to 2 corresponding to the transition at 950 K. The diffusivity $(\gamma) = 1$ corresponds to the normal Curie-Weiss type relaxor and $\gamma > 2$ implies a typical diffuse phase transition type relaxor [15, 21–24]. Thus, the values of γ in the BNM also indicate the formation of ferroelectric micro domains in BNM.

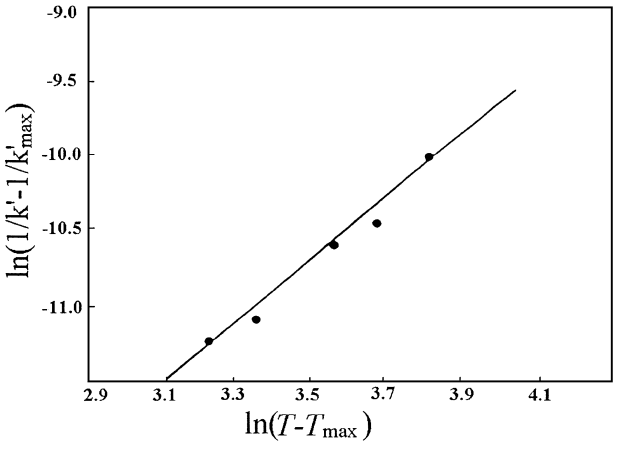

Figure 6 Variation in $\ln(1/k - 1/k_{\max})$ of BNM as a function of $\ln(T - T_{\max})$ at $f = 1$ KHz.

The room temperature resistivity of the sample annealed at 1100 °C is 5.36×10^8 (Ω-cm). However, the sample annealed at 1200 °C has a resistivity 2.94×10^8 (Ω-cm), which is nearly half, and has dielectric constant, which is nearly double that of the former sample. This means that dielectric behavior is closely related to the conduction.

The shapes of the resistivity versus temperature Fig. 7 and loss factor versus temperature Fig. 5 curves are also

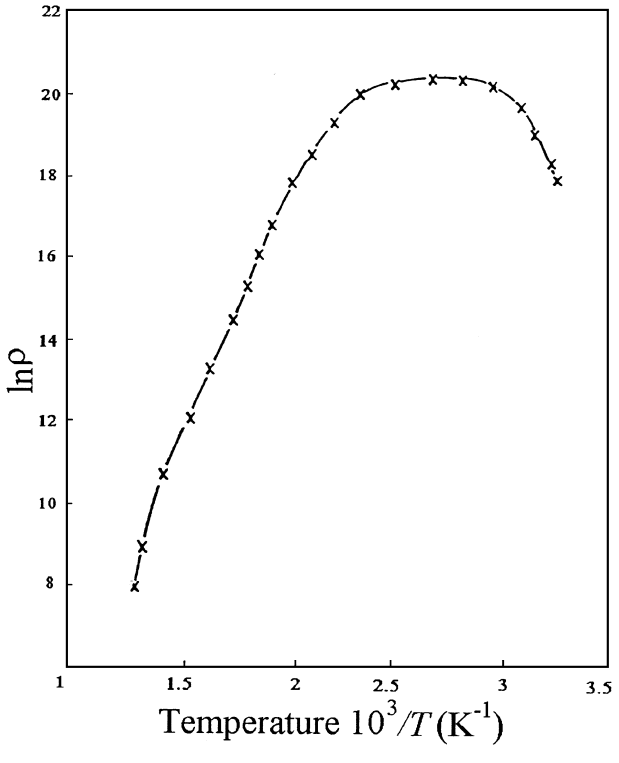

Figure 7 In ρ versus $10^3/T$ for BNM.

compared. They are similar in nature showing that the two phenomena are strongly correlated. The plot of ln ρ versus $1/T$ curve in Fig. 7 of the sample annealed at 1200 °C exhibits a positive temperature coefficient of resistance (PTCR) effect just above the room temperature. The PTCR effect is attributed to the low temperature ferroelectric transition [25, 26]. It can be explained by the Heywang model [27] in the following manner:

The tendency of the Mo^{6+} ion to lower the symmetry is quite obvious from the compounds of the molybdenum [4, 28–30] and the present hexagonal perovskite. Further, the larger size of the Ba^{2+} ion in some barium containing perovskites is known to cause barium vacancies inside the grains [31, 32]. The vacancies would only be enhanced by the presence of smaller Mo^{6+} ions. The larger lattice constants and larger valency of molybdenum ions perhaps imply the ordering of cation vacancies. Thus the lower symmetry of the unit cell and higher ordering of octahedral cations would lead to the polar microdomains inside the grains. Also, as in the case of some barium containing perovskites, the cation vacancies inside the grains are responsible for the *n*-type charge carriers [31, 32]. However, the grain the grain boundaries are deficient of oxygen creating a *p*-type region. This "*p-n* junction" creates potential barrier [27], which may be responsible for the PTCR effect in BNM. At the same higher temperature (850 K), both curves Figs 5 and 7 show discontinuities. Hence, it is concluded that losses are mainly due to conductivity.

The high temperature region of the resistivity curve shows a decrease of resistivity as the temperature increases. This indicates the semiconductor nature of the ceramic. This high temperature region corresponds to intrinsic conduction. It has two activation energies. The low temperature activation energy is 0.89 eV. It increases to 1.32 eV in the high temperature region. The transition is likely to be of order-disorder type. The activation energy is twice the band gap. Thus, the band gap increases from 1.78 eV (order phase) to 2.64 eV (disorder phase).

The I-V characteristic of the BNM ceramic shows a potential barrier (Schottky behavior) in Fig. 8, which is slightly less than 8 eV. Such a large potential barrier may be due to the large band gap of the BNM. These characteristics are compared with those obtained for the $BaTiO_3$ ceramic [33]. The Schottky barrier corresponding to BNM is much higher and the rise in current is not steep.

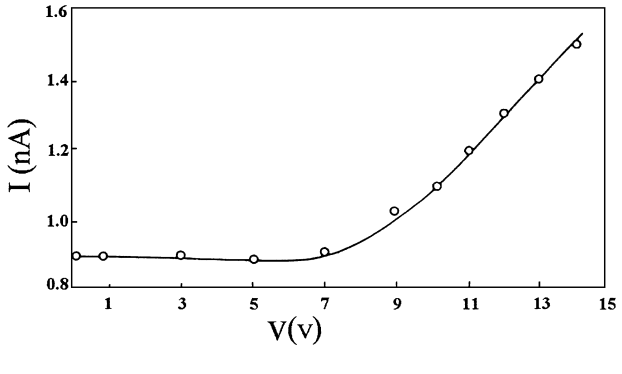

Figure 8 Room temperature I-V characteristics for BNM.

This significant difference between the present ceramic and $BaTiO_3$ is probably due to the high density, very large grain size and appropriate doping of the $BaTiO_3$.

It is concluded that this new perovskite BNM (annealed at 1200 °C) is a diffuse ferroelectric material containing microdomains. It has a positive temperature coefficient of resistance near room temperature. This promising property makes it worthwhile for further investigation.

Acknowledgments

Financial support from Patkar-Varde College and Mumbai University, Mumbai, India is greatly acknowledged.

References

1. P. PAPET, T. R. SHROUT and J. P. DOWHWRTY, *J. Mater. Res.* **5** (1990) 2902.
2. A. S. BHALLA, R. ROY and S. KOMARENI, *Ferroelectr. Lett.* **11** (1990) 137.
3. S. SHARMA, R. N. P. CHOUDHARY, R. SATI and K. P. SHARMA, *Ind. J. Pure Appl. Phys.* **31** (1993) 200.
4. L. H. BRIXNER, *J. Phys. Chem.* **64** (1960) 165.
5. M. F. KUPRIYANOV and E. G. FESENKO, *Sov. Phys. Cryst.* **7** (1962) 358.
6. F. K. PATTERSON, K. MOLLER and R. WARD, *Inorg. Chem.* **2** (1975) 196.
7. A. S. VISKOV, YU. N. VENVTSEV and G. S. ZHDANOV, *SOV. Phys. Dokel.* **10** (1965) 928.
8. S. K. MISHRA and D. PANDEY, *J. Phys. Conden. Matter.* **7** (1995) 928.
9. E. HUSSON, L. ABELLI, L. ABELLOR and A. MORELL, *Meter. Res. Bull.* **25** (1990) 359.
10. G. C. BARRACLOUGH, J. LEWIS and R. S. NYHOLM, *J. Chem. Soc.* **35** (1959) 52.
11. A. R. VAN HIPPEL, "Dielectric and Waves" (John Wiley and Sons Ins., New York, 1954).
12. J. C. MAXWELL, "Electricity and Magnetism," Vol. 1 (Clarendom Press, Oxford, 1982) p. 452.
13. K. W. WANGNER, in "Die Isolierstoffe der Elektrotechnik," edited by H. R. Schering (Springer Berlin, 1924) p. 1 ff.
14. S. SHARMA, R. N. P. CHOUDHARI and R. SATI, *Phys. Status Solidi* (*a*) **133** (1992) 491.
15. J. KUWATA, K. UCHINO and S. NOMURA, *Jpn. J. Appl. Phys.* **21** (1982) 1298.
16. H. D. MAGAW, "Ferroelectricity in Crystals" (Methun, London, 1957).
17. V. S. DHANANJAI, D. PANDEY and V. S. TIWARI, *J. Amer. Ceram. Soc.* **77**(7) (1994) 1819.
18. V. W. KANZING, *Phys. Acta.* **24** (1951) 175.
19. H. T. MARTIORENA and J. C. BURTOOT, *J. Phys.* C **7** (1974) 3182.
20. F. W. COOKE, R. C. BRADT, R. C. DE VRIES and G. S. ANSELL, *J. Amer. Ceram. Soc.* **49** (1966) 648.
21. S. W. CHOI, T. R. SHROUT, S. J. JANG and A. S. BHALLA, *Ferroelectrics* **100** (1966) 29.
22. G. A. SMOLENSOKII, *J. Phys. Soc. Jpn.* **28** (1970) 26.
23. P. GROVES, *J. Phys.* C **19** (1986) 111.
24. H. NEUMANN, G. ARLT, *Ferroelectrics* **69** (1986) 179.
25. J. G. FOGAN, VASANTHA and R. W. AMARAKOON, *J. Amer. Ceram. Soc.* **72**(2) (1993) 69.
26. I. P. RAEVSKII, *Sov. Phys. Solid State* **28**(10) (1983) 1375.
27. W. HEYWANG, *Solid State Electron.* **3** (1) (1961) 57.
28. A. F. WELL, "Structural Inorganic Chemistry," 5th ed. p. 558.

29. F. K. PATTERSON, C. W. MOLLER and R. WAREL, *Inorg. Chem.* **2** (1975) 196.
30. G. BLARSE, *Inorg. Nucl. Chem.* **34** (1972) 3401.
31. V. M. GWZEVICH, Electric Conductivity of Ferroelectric, Israel Program for Scinentific Translation Ltd. IPST cat. No. 5915 (1971).
32. K. SAMBASIVA RAO, *Ind. J. Pure Appl. Phys.* **21** (1993) 43.
33. DA. YU WANG, *J. Amer. Ceram. Soc.* **77** (1994) 897.

Received 8 July
and accepted 24 October 2003